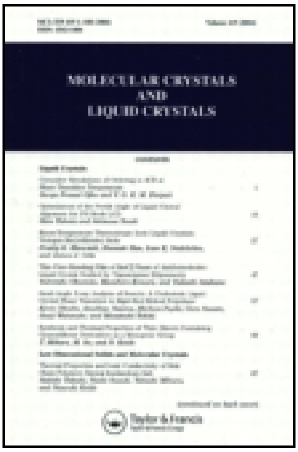

Molecular Crystals and Liquid Crystals
Publication details, including instructions for authors and subscription information:
http://www.tandfonline.com/loi/gmcl16

Structure of the Short Range Ordered Nematic Phases of nBABA (n = 1 to 9

A. S. Paranjpe [a b] , K. Usha Deniz [a b] , P. S. Parvathanathan [a b] , V. Amirthalingam [a c] & K. V. Muralidharan [a c]
[a] Bhabha Atomic Research Centre, Trombay, Bombay, 400 085, India
[b] Nuclear Physics Division
[c] Water Chemistry Division

Version of record first published: 28 Mar 2007.

To cite this article: A. S. Paranjpe , K. Usha Deniz , P. S. Parvathanathan , V. Amirthalingam & K. V. Muralidharan (1987): Structure of the Short Range Ordered Nematic Phases of nBABA (n = 1 to 9, Molecular Crystals and Liquid Crystals, 149:1, 79-101

To link to this article: http://dx.doi.org/10.1080/00268948708082972

Mol. Cryst. Liq. Cryst., 1987, Vol. 149, pp. 79–101
Photocopying permitted by license only

Printed in the United States of America

Structure of the Short Range Ordered Nematic Phases of nBABA (n = 1 to 9)

A. S. PARANJPE,† K. USHA DENIZ,† P. S. PARVATHANATHAN,†
V. AMIRTHALINGAM‡ and K. V. MURALIDHARAN‡

Bhabha Atomic Research Centre, Trombay, Bombay-400 085, India

(*Received June 7, 1986; in final form April 3,1987*)

X-ray diffraction measurements have been carried out on the nematic phase of nBABA (n = 1 to 9). Our results show that this nematic phase is a fibre type one having in addition to the orientational long range order, two types of short range orders, (SROs): (i) one dimensional correlations of the molecular dimers along the nematic director ($\hat{n}$) and (ii) S_C type SRO. The strength of 1-d correlation increases with increasing n for $1 < n \leq 3$ and decreases for $n > 6$. The n-dependence of the length of the correlated units shows that the chains are disordered for large n. The S_C type order which is negligible for $n < 3$, strengthens with increasing n. The corresponding correlation length (ξ_2) is found to be asymmetric with $\xi_{2\parallel}(\parallel\hat{n}) > \xi_{2\perp}(\perp\hat{n})$. This asymmetry decreases with increasing n. The formation of the observed structures in the SROs has been qualitatively explained taking into account various types of intermolecular interactions.

Keywords: liquid crystals, nematics, short range order, X-ray diffraction

INTRODUCTION

The compounds nBABA (Figure 1) exhibit[1] only nematic liquid crystalline phases for $1 \leq n \leq 5$, but for $6 \leq n \leq 9$ they exhibit both, the nematic (N) as well as the smectic C (S_C) phases. It is found that the molecules form dimers in both the liquid crystalline phases.[2,3] It is thought that the dimers are of the closed type, making the rigid portion of the molecule fairly long (≈29.0Å). The nematic phases for the members n = 1 to 7 have, in addition to the long range orien-

---

†Nuclear Physics Division
‡Water Chemistry Division

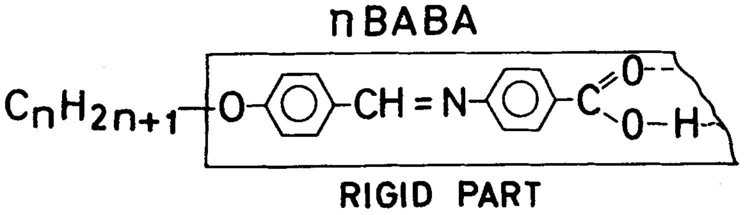

FIGURE 1 nBABA molecule.

tational order, short range ordered (SRO) regions having (1) S_C type order, like the skewed cybotactic nematics (N_{SC})[4] and (2) 1-dimensional (1-d) correlation of the molecules along the nematic director ($\hat{n}$). These nematics are designated, "fibre type nematics" (N_F).[5] For $n > 7$, the 1-d correlation is not seen whereas S_C type SRO is very strong. This paper describes the results of x-ray diffraction measurements which have been carried out in the nematic phase of nBABA for $n = 1$ to 9, to study the behaviour of the SROs as a function of chain length. From our results, the intermolecular distance (D) perpendicular to $\hat{n}$, length of the 1-d correlated units (L_{CU}), interplanar distance in the cybotactic groups (d_R) and the correlation lengths in both types of SROs are obtained as a function of n. The variations of the strengths of these SROs as a function of n are discussed in terms of various intermolecular interactions such as the dipolar and chain–chain interactions. A model for the molecular conformation has been built, which shows some interesting features.

EXPERIMENTAL FEATURES

The apparatus used in the present work has been described in detail elsewhere.[3] Ni filtered Cu radiation and a Laue camera were used in the experiments. Samples were contained in capillaries and were aligned along the capillary axis in a magnetic field of about 0.16 T. Diffraction photographs were taken at a temperature $T \approx T_{tr} + 0.5°C$. T_{tr} is the temperature for the transition to the nematic phase from the low temperature phase. The temperature stability was ±0.5°C during the exposure time (two hours) for each photograph.

RESULTS

The evolution of the nematic structure as the chain length increases, can be seen from the x-ray diffraction photographs in the N_F phase of nBABA (Figure 2). Figure 3 gives the schematic representation of the diffraction pattern in this phase. The following features can be noticed in the photographs. (1) Two pairs of diffuse arcs are observed along the equator (perpendicular to $\hat{n}$). The outer ones are related to the average intermolecular distance,[4] D. The inner arcs are due to the incident beam not being monochromatic. This is in-

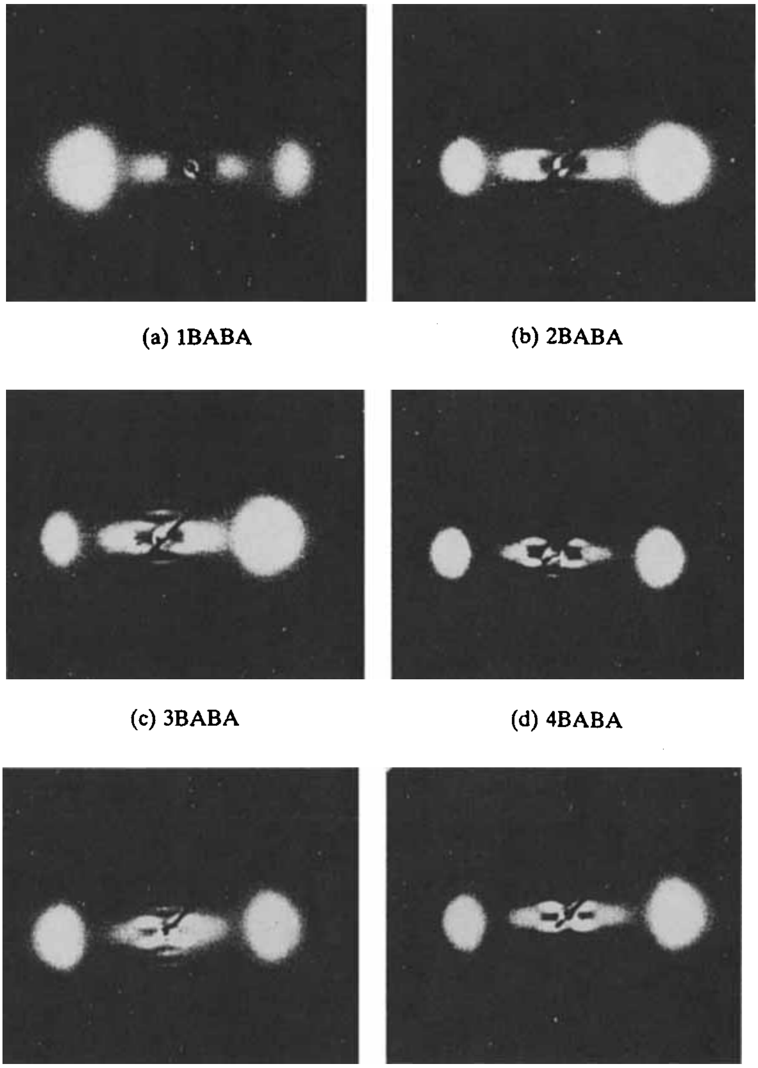

(a) 1BABA (b) 2BABA

(c) 3BABA (d) 4BABA

(e) 5BABA (f) 6BABA

FIGURE 2 X-ray diffraction photographs in the nematic phase of nBABA (n = 1 to 9).

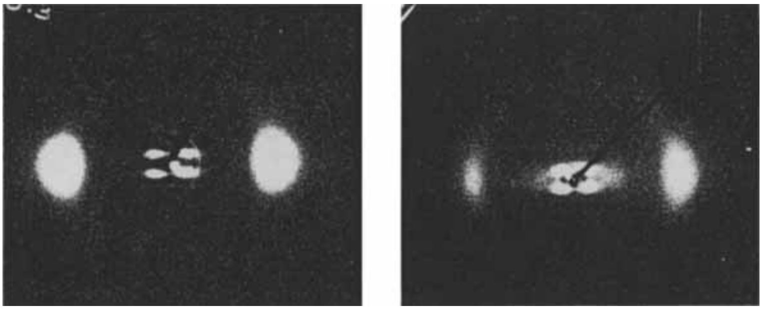

(g) 6BABA (h) 7BABA

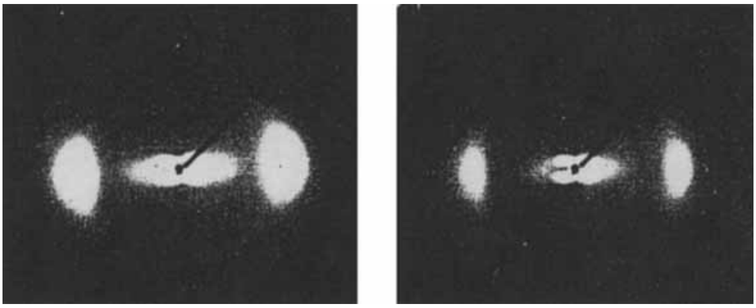

(i) 8BABA (j) 9BABA

FIGURE 2 (*continued*)

dicated by their absence in the photograph for 6BABA (Figure 2g) taken with a monochromatic beam.[6] (2) Along the meridian ($\parallel \hat{n}$) there are a number of diffraction lines running perpendicular to $\hat{n}$ (Figure 3). These lines seem to be due to layers of diffraction caused by 1-d correlation of molecular units along $\hat{n}$. Such type of correlations have been observed in the nematic phase of TBEA[7] and also in some of the ordered smectic phases.[8] The intensity of these diffraction lines increases as n increases from 1 to 3, stays strong for $3 \leq n \leq 5$, and decreases thereafter, almost disappearing for $n \geq 8$. The maximum number of these lines is seen for $n = 3$. The relative intensities of the different lines also changes as a function of n. (3) Four diffuse spots are seen at small angles due to diffraction from S_C type SRO regions. These spots are anisotropic, their width perpendicular to $\hat{n}$ being larger than that parallel to $\hat{n}$. The intensity and the sharpness of these spots increase whereas their anisotropy decreases with increasing n. For $n < 4$ these spots are almost linear and quite weak

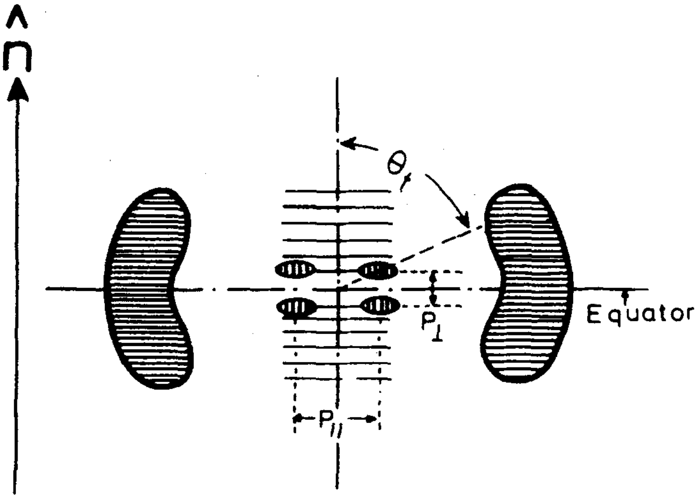

FIGURE 3 Schematic representation of x-ray diffraction pattern for the nematic phase of nBABA.

and diffuse. The diffraction patterns of these nematics (specially of those in which 1-d correlation is strong) resemble to a great extent the diffraction patterns obtained with fibres. Hence the designation 'fibre-type' nematic (or N_F) to distinguish these nematics from the skewed cybotactic nematics (N_{SC}).

The diffraction patterns have been analysed using a microdensitometer. We have obtained (1) D, the average intermolecular distance, $\perp$ to $\hat{n}$, (2) the intensities and the widths of the meridional lines and the corresponding lattice spacing d_m (m = layer order) and (3) from the cybotatic spots we have obtained (a) their intensity, I_{SRO}. (b) their widths parallel and perpendicular to $\hat{n}$ ($w_\parallel$ and $w_\perp$) (c) the interplanar distance, d_R and (d) the molecular tilt angle (θ_t).

The Bragg condition was used to calculate d_m and d_R while D was obtained using de Vries[4] relation. θ_t was measured directly from the photographs (θ_{td}) as also calculated using the relation, $\tan\theta_{tc} = P_\perp / P_\parallel$ (Figure 3). The length, L, of the molecular dimer was calculated assuming an extended zig-zag conformation of the chains.[9]

The measured widths of the cybotactic spots, θ_t and d_R are highly inaccurate for $n \leq 3$ due to the diffuse nature of the spots, w and θ_t being almost impossible to measure in these three members. The errors have been estimated to be about 3 percent in d_m (for $n < 7$) and D, 10 percent or more in the intensities, widths and θ_t and about 6 percent in d_R for $n > 3$.

DISCUSSION

Equatorial maxima and the intermolecular distance (D)

Figure 4 shows the intensity contour maps of the diffuse peak for 1BABA and 9BABA. The peak shapes are quite different in the two compounds. In 1BABA, the orientational order is so large that the shape of the maximum seems to be determined more by the molecular form factor than by the orientational order, whereas for 9BABA, it is the latter which seems to be the determining factor. The diffuse peaks for $n \leq 6$, are similar to those of 1BABA and their angular full width at half maximum, $\Delta\theta$, is in the range, $30° < \Delta\theta < 42°$. For $n > 6$, the peaks resemble those of 9BABA which, in turn, resemble those of normal nematics in which $\Delta\theta$ can be clearly related to the orientational disorder (fluctuations) of the nematics.[10] Thus for $n \leq 6$, the orientational long range order (S) of the rigid portions is quite large. Table I gives the values of $\Delta\theta$ as a function of n and also of the corresponding reduced temperature, T/T_{NI}. From this it would seem that $\Delta\theta$ and hence S is not just dependent on the reduced temperature, T/T_{NI}, but that the presence of 1-d correlation also seems to contribute to this enhancement. From these diffuse maxima we can deduce that the chain axes do not seem to be ordered at least for $n \leq 6$. If the chains were ordered, they would also have contributed to the outer diffuse maxima, in the form of tails as observed in the S_C phases of nBABA[11] and in the nematic phase of 40BA.[12]

The values of D for the nine members have been given in Table II. It is found that D hardly changes with n, showing that even for

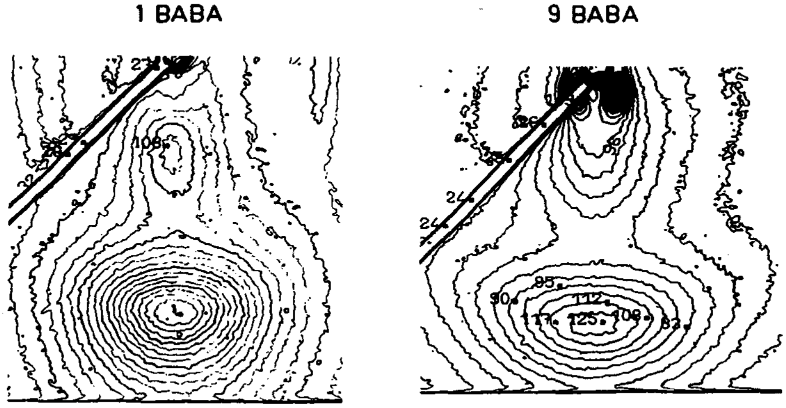

FIGURE 4 Intensity contour maps of the equatorial diffuse peaks for 1BABA and 9BABA.

TABLE I

The reduced temperature, T/T_{NI} and $\Delta\theta$ as a function of *n*

n	T/T_{NI}	$\Delta\theta(°)$
1	0.84	42.5
2	0.84	36.0
3	0.89	34.0
4	0.84	31.0
5	0.84	33.5
6	0.86	31.5
7	0.92	53.0
8	0.94	57.0
9	0.96	65.0

the members with longer chains, disorder in the chains, if present, is not sufficiently large to necessitate a larger intermolecular separation.

1-d correlation

The lattice spacing d_m and the relative intensities I_m of those meridional layer lines which could be separated from the background are also given in Table II. For any particular layer line, m was chosen so that the value of md_m would be as close as possible to L. m = 1

TABLE II

D, d_m and I_m for nBABA (*n* = 1 to 9)

n	1	2	3	4	5	6	7	8	9
D(A)	5.07	5.04	5.06	5.05	5.04	5.02	5.06	5.01	5.10
d_1	—	—	—	41.5	40.4	42.2	38.8	—	—
I_1	—	—	—	39	61	—	—	—	—
d_2	16.9	17.8	18.3	19.4	19.9	21.1	22.0	21.1	—
I_2	25	76	100	100	100	100	92	56	—
d_3	11.1	11.8	12.4	13.0	13.4	13.8	12.9	—	—
I_3	31	66	61	56	62	66	65	—	—
d_4	7.6	8.3	8.8	9.3	—	—	—	—	—
I_4	100	100	56	23	—	—	—	—	—
d_6	—	—	6.8	6.5	6.6	6.8	7.2	7.4	7.7
I_6	—	—	18	19	37	81	100	100	100
d_7	—	5.0	5.1	5.5	5.5	—	—	—	—
I_7	—	48	63	43	52	—	—	—	—
d_8	—	4.3	4.6	—	—	—	—	—	—
I_8	—	27	34	—	—	—	—	—	—

[a] We have not given any values for I, where it was very difficult to separate the signal from the background.

to 4 refer to the corresponding observed meridional lines, whereas m = 6 to 8 refer to the fifth, sixth and seventh observed lines. We can see from the results that the layer lines corresponding to m = 2 and 3 result from the 1-d correlation of molecular units of length md_m ($2d_2 \approx 3d_3$, for *n* = 1 to 6) which is nearly equal to L. For *n* = 7, $3d_3 < 2d_2$ but $2d_2 \approx$ L. This could be due to a large weakening of the 1-d correlation. The line for m = 4, although not connected with the same correlated unit, still depends upon the molecular length (d_4/L ≈ 0.23). d_6 (corresponding to the fifth observed layer line, whose origin is not understood) is almost constant ($\approx$ 6.6Å) for *n* = 3 to 6, but increases for $n > 6$. d_7 and d_8 could be the 7th and 8th order layer lines for the correlated units of d_2 and d_3 since $7d_7 \approx 8d_8 \approx 2d_2$. The lines for $m \geq 6$ are unlike the ones for $m < 6$ in that they are not linear but curved, showing that they are not strictly related to any 1-d correlation.

The length, L_{CU}, of the 1-d correlated units giving rise to the second and third lines has been calculated using the relation, $L_{CU} = (2d_2 + 3d_3)/2$ except in the case of 7BABA and 8BABA where it has been taken as $2d_2$. L_{CU} and L are shown as a function of *n* in Figure 5. L shows an odd–even effect, whereas this effect is negligible (see dashed line in Figure 4) in L_{CU}. Surprisingly, L_{CU} is almost linear in *n*, and is always less than the corresponding L except in 1BABA. If the

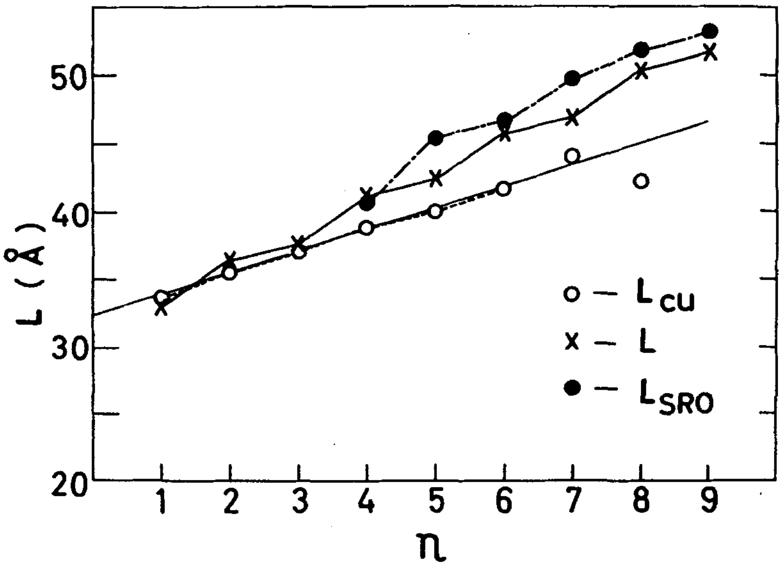

FIGURE 5 The lengths L, L_{CU} and L_{SRO} as a function of *n*. The straight line going through the L_{CU} points is a visual guide.

molecular dimers are the correlated units, then this implies that the molecules are not in the extended conformation and there is a disordering of the chains which leads to the disappearance of the odd-even effect.

The intensities I_m show rather interesting features: (1) For $n = 1$, the highest intensity is I_4. As n increases, this intensity decreases showing that the correlation giving rise to this line weakens, disappearing for $n > 4$. (2) The intensity I_2 increases with increasing n for $1 < n < 3$ and is the largest layer line intensity for $n = 3$ to 6, beyond which it decreases. This again shows that the 1-d correlation giving rise to lines 2 and 3 increases in strength for $1 \le n \le 3$, is strong for $n = 3$ to 6 and then dies off for $n > 6$. (3) As stated earlier, the fifth line ($m = 6$) is not related to any 1-d correlation for $3 < n \le 5$. For $n > 5$, it could be related to some correlated unit which is not the molecular dimer. The strength of this line builds up with increasing n for $n > 4$, showing that probably the S_C type SRO is responsible for this line.

It should be noted that the position of the layer lines and their relative intensity, I_m, are not only governed by the fibre-type structure (1-d correlation) of the molecules but are also dependent on the molecular form factor which is determined by the molecular conformation.

The widths of the layer lines have been measured wherever possible and the 1-d correlation lengths, ξ_1, $\parallel \hat{n}$ have been calculated using the Scherrer relation[13]

$$\xi_1(m) = 2/\Delta Q(m)$$

where $Q = k/2\pi = (2\sin\theta)/\lambda$, $\mathbf{k}$ is the scattering vector (see Figure 8) and $\Delta Q(m)$ is the full width at half maximum of the mth line. $\xi_1(m)$ is plotted as a function of m for various n in Figure 6. For $n = 2$ to 6, $\xi_1(m)$ decreases with increasing m (see hatched area in Figure 6). $n = 1$ is an exception to this case and for $n > 6$ the number of reflections are very few to draw any conclusions. The number of correlated units, taken as $\xi_1(2)/L_{CU}$ turns out to be about 5 for $n = 2$ to 6. $\xi_1(m)$ for m = 2, 3 and 6 have also been plotted as a function of n (in Figure 7). In addition to the fact that $\xi_1(2)$ and $\xi_1(3)$ fall off sharply for $n = 1$ and 7 there is an interesting odd–even effect, and a peaking of the correlation lengths at $n = 4$. Given for comparison is the n-dependence of the nematic to isotropic transition entropy, ΔS_{NI}.[14] It is interesting to note that although a sharp fall for $n = 1$ and 7 is not shown by ΔS_{NI}, its n-dependence resembles that of $\xi_1(2, 3)$ since it also shows an odd–even effect and a peaking at $n = 4$.

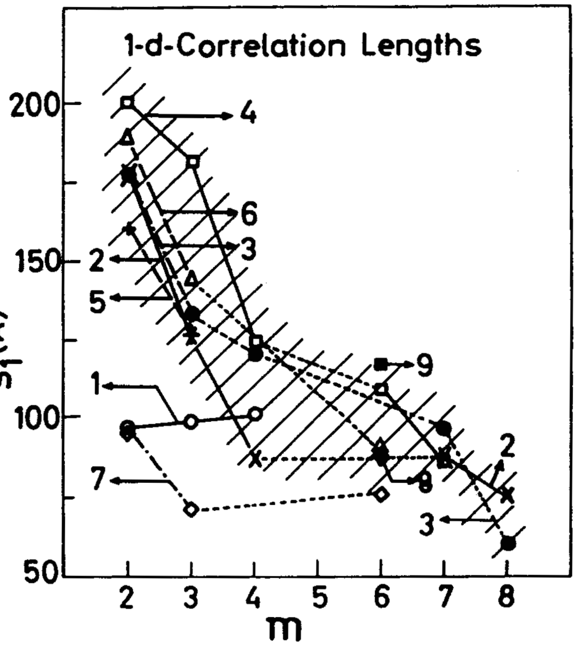

FIGURE 6 ξ_1 as a function of m for different n. ○: $n = 1$, ×: $n = 2$, ●: $n = 3$, □: $n = 4$, +: $n = 5$, △: $n = 6$, ◇: $n = 7$, ◆: $n = 8$, ■: $n = 9$.

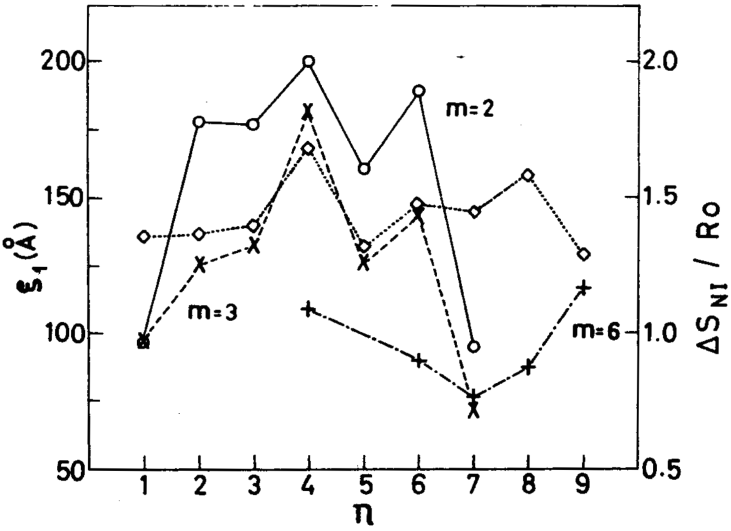

FIGURE 7 n—dependence of $\xi_1(2)$, $\xi_1(3)$, $\xi_1(6)$ and of the transition entropy, $\Delta S_{NI}/R_0$, where R_0 is the gas constant. ○: $\xi_1(2)$, ×: $\xi_1(3)$, +: $\xi_1(6)$, ◇: $\Delta S_{NI}/R_0$.

This could mean that the NI transition involves breaking up of the 1-d correlation, which makes a significant contribution to ΔS_{NI}. This would then explain the rather high values of the observed ΔS_{NI} as compared to the values obtained for ordinary nematics and also that calculated by Maier-Saupe theory.[15] The reason for ΔS_{NI} not decreasing for $n > 6$ could be because the S_C type SRO which increases in these members might breakdown at T_{NI}, thus contributing to ΔS_{NI}. $\xi_1(6)$ shows a trend which is completely different from that of the other two and increases with increasing n for $n \geq 7$. This confirms that for this range of n, the fifth line is related to S_C type order.

1-d correlation of molecules has been observed[8] in several ordered smectic phases and even in the crystalline phase of TBBA. Doucet,[8] in an exhaustive study of the S_G phases of several compounds by X-ray diffraction, has found meridional layer lines resulting from the existence of strings of molecules correlated along their long axes. The correlation length along the string, extended up to about 10 molecules in some cases (40.2 and TBBA). This string-like structure in a highly (almost 3-dimensionally) ordered smectic phase is attributed to the displacement, say $\mathbf{U}$, of molecules from their mean positions; the molecules of the same string are activated by the collective longitudinal movements, $\mathbf{U}_L$ and the individual transverse movements $\mathbf{U}_T$, the latter leading to a broadening (|| string) of the meridional lines, as one moves away from the meridian. The intensity of the layer lines is then proportional to $\sin^2(\mathbf{q}\cdot\mathbf{U}_L)$, and it is also dependent on the molecular form factor. The extent (Δ_L) to which the meridional layer lines are observed in the reciprocal space is, therefore, related to the displacement by, $U_L \sim 1/\Delta_L$. Doucet observed that, (a) this correlation declines in strength as the end chain length increases, and (b) there are no such correlations found in the S_A and S_C phases of TBBA.

There are similarities between Doucet's results and our observations: (1) We have not observed any meridional lines for the S_C phases of nBABA that we have studied ($n = 6$ to 9). (2) In the nematic phase also, the layer lines become weaker and less in number as the chain length increases. Doucet's model cannot be used in the case of nematics since they do not possess positional long range order. A possible explanation for the observed string formation (1-d correlation) in the case of the nematics that we have studied, is given later.

The S_C type SRO (correlations)

The nematics exhibiting S_C type short range order (skewed cybotactic nematics) are often preceded by a low temperature S_C phase, though this is not so always (e.g. 5BABA). In the latter case, the SRO is not very strong and could result from a tendency to form a low temperature S_C phase, a tendency which is overwhelmed by other forces, leading to the formation of a 3-dimensionally ordered phase, instead.

In the x-ray diffraction pattern from a skewed cybotactic nematic (near the N−S_C transition) one observes four diffuse spots instead of the two meridional arcs seen for ordinary nematics. This arises from the fact that the scattering from a skewed cybotactic nematic is concentrated on two rings in the reciprocal space (Figure 8), defined by the scattering vector, **k**, given by,

$$\mathbf{k} = \mathbf{k}_i - \mathbf{k}_s = \mathbf{q}_0 \tag{1}$$

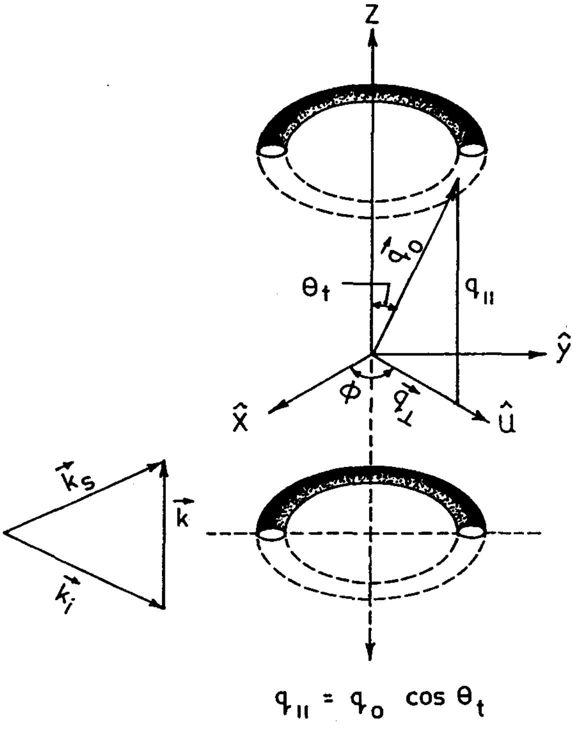

FIGURE 8 Vector diagrams representing Eqs. (1) and (2). The rings indicate the regions in reciprocal space where X-ray diffraction maxima are expected. The ring cross-section (see cut-off section) is elliptical showing that the observed diffuse X-ray spots are anistropic.

where $\mathbf{k}_s$ and $\mathbf{k}_i$ are the scattered and incident X-ray wave vectors, with $k_s = k_i = 2\pi/\lambda$. $\mathbf{q}_0$ is a vector perpendicular to the smectic planes and its magnitude is $2\pi/d_R$.

$$k_z = q_{\parallel} = q_0 \cos\theta_t \quad \text{and} \quad (k_x^2 + k_y^2)^{1/2} = q_{\perp} = q_0 \sin\theta_t \tag{2}$$

One can picture this nematic as containing S_C droplets wherein the nematic director $\hat{n}$ is fixed parallel to the z-axis. The magnitude, θ_t, of the tilt angle is also fixed, but the direction of the tilt, φ, varies from droplet to droplet (Figure 8) and can take any value between 0 and 2π. Using this model, the S_C-type SRO in a nematic in the vicinity of the $N-S_C$ transition has been considered in detail, theoretically, by de Gennes,[16] Chu and McMillan (CM),[17] and Chen and Lubensky (CL).[18] Their theories use the Landau type expansion for the free energy in terms of the S_C order parameter(s). In the theories of de Gennes and CL, the smectic C order parameter, ψ, refers to the mass density wave with fundamental wave number q_0 ($\mathbf{q}_0 \equiv$ q $\cos\varphi$, q $\sin\varphi$, $q_{\parallel}$). On the other hand, CM theory uses two order parameters, (a) the smectic order parameter, ψ, referring to a mass density wave in the $x-z$ plane with fundamental wave number q_0, and (b) the orientational order parameter, $\boldsymbol{\beta} = \beta_0\hat{x}$, where $\beta_0 = \tan\theta_t$, pictured as the average electric dipole moment per molecule. In all three theories, the free energy expression is such that the Landau rules allow a second order $N-S_C$ phase transition. However Brazowskii[19] has shown that such transitions are first order due to large fluctuations in the order parameter. Nevertheless, the pretransitional effects could be important (our X-ray diffraction results show this to be the case) and hence the predictions of the theories of de Gennes, CL and CM are of interest. We will give below their expressions for the scattered X-ray intensity in the vicinity of the rings.

(a) de Gennes' theory (neglecting the cross term)

$$I(\mathbf{k}) = \int \frac{d\varphi}{\alpha + (k_z - q_{\parallel})^2/2M_V + (\hat{u}\cdot\mathbf{k}_{\perp} - q_{\perp})^2/2M_T} \tag{3}$$

where $\hat{u} = \hat{x}\cos\varphi + \hat{y}\sin\varphi$, a unit vector in the plane perpendicular to $\hat{n}$, and $k_{\perp}$ is given by, $k_{\perp}^2 = k_x^2 + k_y^2$. M_V and M_T can be thought of as components of a mass tensor and are coefficients of the gradient term in the free energy expression. The correlation lengths, $\xi_{2\parallel}(\parallel\hat{n})$ and $\xi_{2\perp}(\perp\hat{n}$ and $\parallel\hat{u})$ are given by,

$$\xi_{2\parallel} = (2M_V\alpha)^{-1/2}, \qquad \xi_{2\perp(\parallel\hat{u})} = (2M_T\alpha)^{-1/2} \tag{4}$$

but $\xi_{2\perp(\perp\hat{u})}$ is reduced and is $\sim(\xi d_R)^{-1/2}$. Using mean field theory, $\alpha \sim (T - T_{NC})$. Hence,

$$\xi_{2\parallel,\perp(\parallel\hat{u})} \sim (T - T_{NC})^{-1/2} \tag{5}$$

(b) CL theory

$$I(k) \sim \frac{1}{\bar{a} + D_{\parallel}(k_z^2 - q_{\parallel}^2)^2 + D_{\perp}(k_{\perp}^2 - q_{\perp}^2)^2} \tag{6}$$

where $\bar{a} = a'(T - T_{NC})/T_{NA}$. a', $D_{\parallel}$ and $D_{\perp}$ are related to coefficients in the free energy expression. Here again the two correlation functions, $\xi_{2\parallel}$ and $\xi_{2\perp(\parallel\hat{u})}$ are given by Eq. (5) as would indeed be expected of an MFT calculation.

(c) CM theory

$$I(k) = \frac{k_B T}{[\{a + C_{\parallel}(k_z - q_{\parallel})^2 + C_{\perp}(k_{\perp} - q_{\parallel}\beta_0)^2\}^{1/2} * \{a + C_{\parallel}(k_z - q_{\parallel})^2 + C_{\perp}(k_{\perp} + q_{\parallel}\beta_0)^2\}^{1/2}]} \tag{7}$$

where a, $C_{\parallel}$ and $C_{\perp}$ are related to some of the coefficients in the free energy expansion. Eq. 5 holds good in this case also. CM had found that their theory rather than de Gennes' agreed with earlier x-ray diffraction results. However, recent high resolution x-ray scattering results[20] are found to agree very well with CL's predictions and not with those of CM.

The accuracy of our measurements does not justify line shape comparisons with the above theoretical predictions. Hence while analysing our results we have only measured the widths at half maxima of the SRO peaks and used them as a measure of the inverse correlation lengths. This is justified in the case of de Gennes' theory but not in the case of the other two theories (see Eqs. 6 and 7). The correlation lengths $\xi_{2\parallel}$ and $\xi_{2\perp}$ for this SRO, have been calculated using the widths of the spots, in the same way as for $\xi_1(m)$, and they are shown in Figure 9. It should be noted that this $\xi_{2\perp}$ is not $\xi_{2\perp(\parallel\hat{u})}$ (Eq. 4). It is found that $\xi_{2\parallel}$ is almost independent of *n* whereas $\xi_{2\perp}$ increases with increasing *n*. Thus ξ_2 becomes less anisotropic with increasing *n*. Our results show that the extent of the cybotactic group (in terms of the

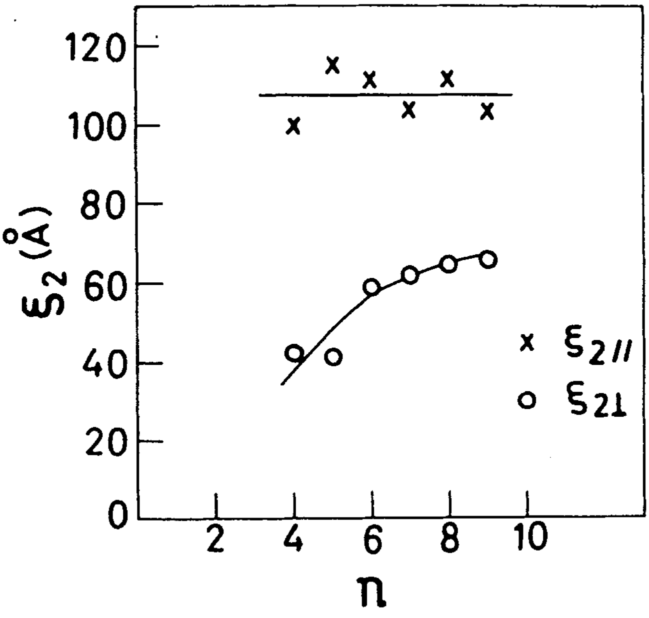

FIGURE 9 *n* dependence of $\xi_{2\parallel}$ and $\xi_{2\perp}$. Lines are visual guides.

number of molecules) hardly changes ∥ to $\hat{n}$ (2 to 3 dimer units), whereas ⊥ to $\hat{n}$, it increases with increasing *n* (from about 8D for n = 4 to about 13D for n = 9). A pictorial representation of this is seen in Figure 10. In the light of de Gennes' theory (see Eq. 4) this would mean that the ratio M_T/M_V decreases as *n* increases. Our values

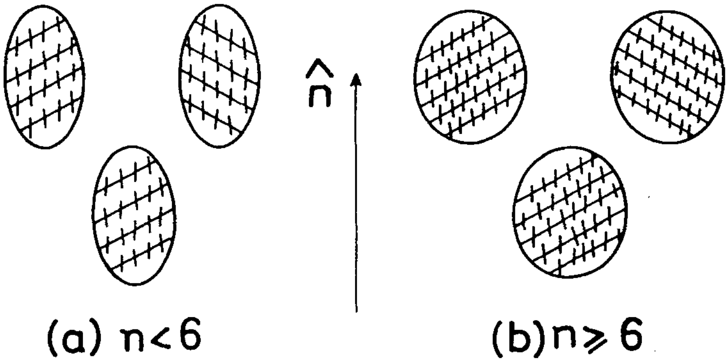

FIGURE 10 Pictorial representation of the molecular arrangement in the cybotactic groups.

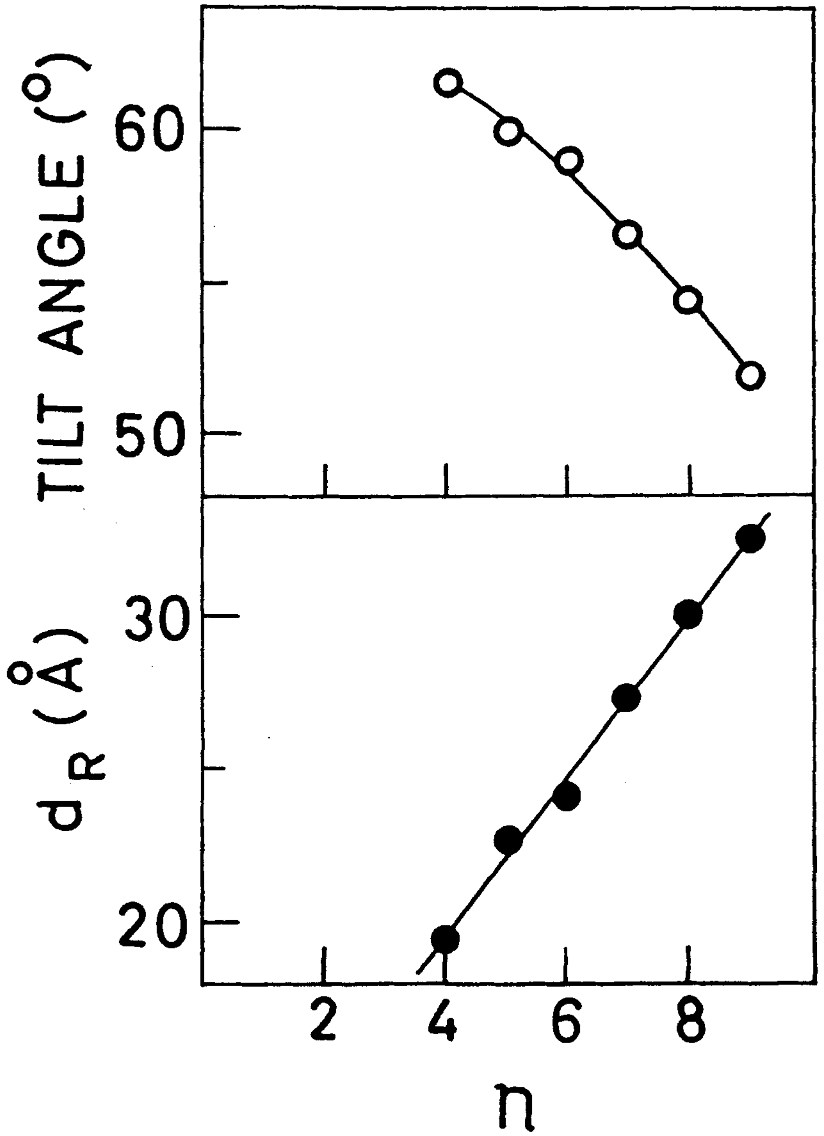

FIGURE 11 Layer thickness, d_r and tilt angle θ_t as a function of *n*. Lines are visual guides.

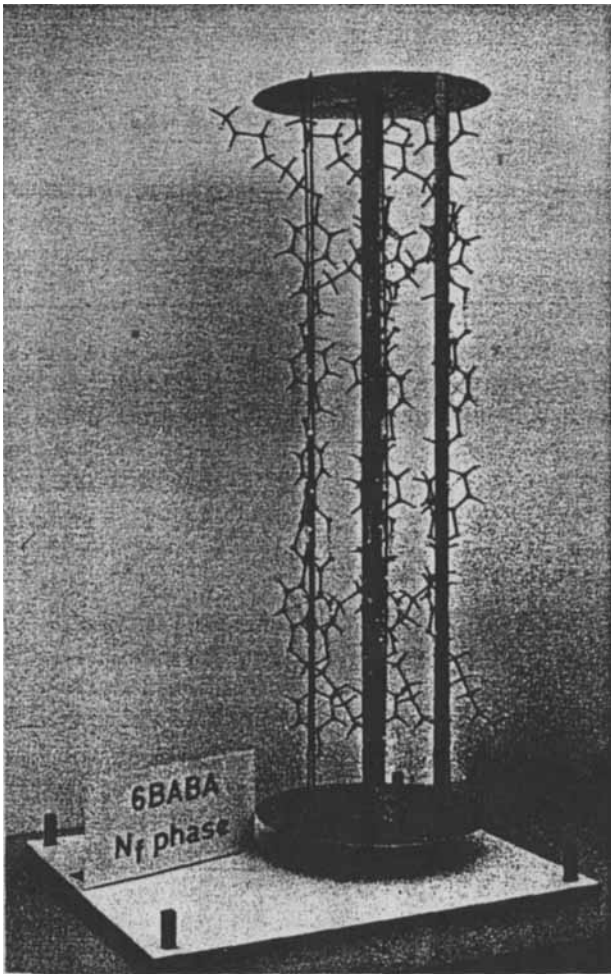

FIGURE 12 Photograph of the model for 6BABA.

of $\xi_{2\parallel}$ and $\xi_{2\perp}$ represent only a lower limit on their actual values, since the cybotactic spots are also broadened by the thermal fluctuations in the orientational order parameter.

The values of d_R obtained from our results are found to increase with increasing *n* (Figure 11). The value of the molecular length, L_{SRO}, calculated using the relation $L_{SRO} = d_R/\cos\theta_t$ is shown in Figure 5. We find that $L_{SRO} > L$ for $n > 4$. It also shows an odd–even effect opposite to that of L. We are not able to explain the observed behaviour of L_{SRO}. It is found that $\theta_{tc} \approx \theta_{td}$ in all cases. Hence we have only plotted the latter as a function of *n* in Figure 11. θ_t is found

TABLE III

θ_t in the S_C and the nematic phases

n	θ_t(N)	θ_t(S_C)
6	59.0	55.2
7	56.6	50.0
8	54.5	49.2
9	52.0	47.5

to decrease monotonically with increasing n. The values of the tilt angles for $n = 6$ to 9 measured in the nematic phase in the present experiments and those measured in the S_C phase for $T \approx T_{CN} - 2°C$,[3] have been given in Table III. In all cases, there is an increase of θ_t in the nematic phase. This trend is opposite to that observed by Chu and McMillan for HAB.[17]

Model for the nematic phase

A model (see Figure 12) was constructed to examine the packing of nearest neighbour molecules in the nematic phase. It was assumed that (1) the molecules were in a zig-zag conformation with their long axes parallel to the line joining the centres of the benzene rings in a

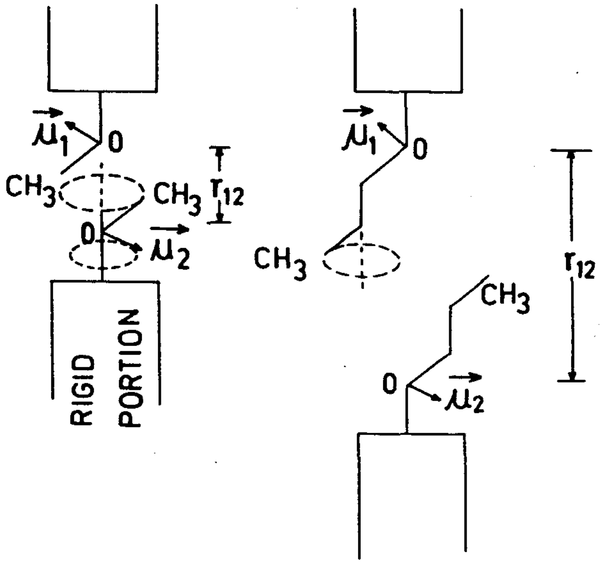

FIGURE 13 Schematic representation of interactions between the terminal dipoles μ_1 and μ_2.

monomer, (2) the nearest neighbour (nn) molecules were packed in a hexagonal fashion, perpendicular to their long axes (taken to be $\parallel \hat{n}$) with nn distance $\perp \hat{n}$ being 5 Å, (3) the centres of mass of the nn molecules lie in a plane whose perpendicular is at ~60° to $\hat{n}$ and that (4) nn molecules were oriented in the same way. Two interesting features were indicated by this model: (a) a herringbone packing of nn molecules was necessary, as predicted by de Vries[21] and (b) for $n > 3$, the end chains could not be in an all-trans conformation.

Interactions leading to short range ordered structures[3]

It is well known that (i) the Van der Waals forces between the rigid parts of the molecules can account for the long range orientational order,[15] (ii) the chain–chain interactions are important for the formation of smectic phases[22] and that (iii) the dipolar interactions do play an important role in stabilizing the S_C phases.[23,24] We will try to explain qualitatively the short range ordered structures observed in the nematic phases of nBABAs and their variations as a function of n in terms of these interactions.

a. Interactions leading to 1-d correlations. Strong terminal intermolecular interactions $\parallel \hat{n}$ in the nematic phase will lead to 1-d correlation of molecules. These are (i) dipole–dipole interactions (ii) dipole–induced dipole interactions, (iii) induced dipole–induced dipole interactions and (iv) the Van der Waals interactions between the end hydrocarbon chains of neighbouring molecules $\parallel$ to $\hat{n}$.

Contribution to the terminal dipole–dipole interaction would be mainly from the dipoles at the oxygen sites. This interaction can be written as

$$\frac{\mu_1 \cdot \mu_2}{r_{12}^3} - \frac{(\mu_1 \cdot r_{12})(\mu_2 \cdot r_{12})}{r_{12}^5}$$

where μ_1 and μ_2 are the dipoles at the oxygen sites of the neighbouring molecules and r_{12} is the distance between them (Figure 12). Here it is assumed that the distance between the positive and negative charges of each dipole is small compared to the distance between the dipoles. From the above expression we see that (i) the interaction is strong when μ_1 and μ_2 are aligned parallel and (ii) when r_{12} is small. It is well known that the last two to three segments of the end chains of the molecules are quite disordered.[25] Hence, for $n = 1$, there will be no order in the chain segment O—C, i.e. $\langle \mu_i \rangle = 0$. The ordering of μ_i, i.e. of the chain segment O—C, improves with increasing chain length, becoming quite good at $n = 4$. This will also lead to an increase in the induced dipole moment, thus affecting the dipole-induced dipole and induced dipole–induced dipole interactions. There are two opposing effects as n increases—(i) μ_i becomes more ordered leading to a stronger interaction which, however, does not increase with n beyond a certain chain length, and (ii) r_{12} increases, decreasing the interaction. Hence, with increasing chain length, one could expect a maximizing of the interactions at some r_{12} corresponding perhaps to $n = 3$ or 4. Thus the n dependence of the net dipolar interaction would explain the observed behaviour of $\xi_1(2)$ and its maximization at $n = 4$.

It should be noted that nBABA molecules (Figure 1) have long, highly polarizable rigid parts. This high polarizability seems to be one of the major contributors to the large terminal interactions leading to 1-d correlations. In the absence of such long polarizable rigid portions in the molecules, strong 1-d correlations are not observed, as is the case for the alkoxybenzoic acids.[26]

b. Interactions leading to S_C type SRO. Strong lateral ($\perp\hat{n}$) intermolecular interactions will be responsible for this SRO. It should be pointed out that as against the terminal interactions which decrease with n due to increasing intermolecular distance, lateral interactions are not directly affected by variation of n because D is almost constant as a function of n. Two important interactions which can be considered are: (1) interactions between dipoles, which in this case, seem to be between the dipole moments at the oxygen and nitrogen sites of the neighbouring molecules (since $\theta_t \approx 60°$) (Figure 13) and (2) the chain–chain (Van der Waals) interactions. McMillan[17] has predicted that when molecules have outboard dipoles, dipole–dipole interactions between the neighbouring molecules favour the formation of an S_C phase. In the case of nBABA (for $n \leq 3$, the dipoles at the oxygen site are disordered and hence the dipolar interactions are small and the S_C type SRO will be very weak. For $n > 3$ the interactions become quite strong due to the alignment of these dipoles leading to well formed S_C type SRO (cybotactic groups). The chain–chain interactions are negligible for $n \leq 3$ because of the (1) non-overlap of the chains and (2) chain disorder. But the chain overlap increases with the chain length, causing an increased chain–chain interaction and hence an increased chain ordering, the net effect again favouring smectic type order. Hence, due to both the interactions, a

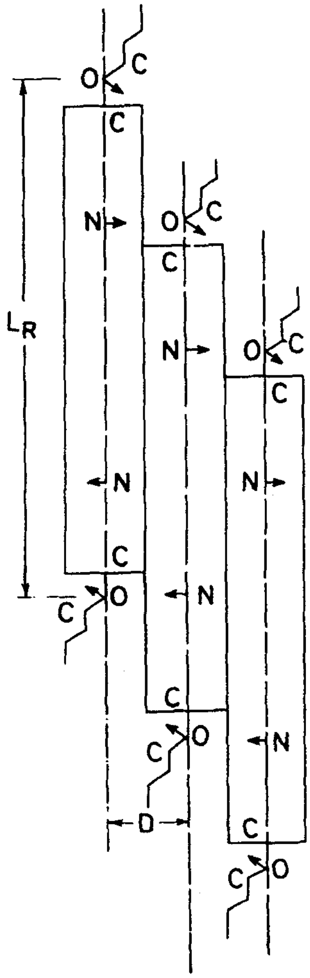

FIGURE 14 Schematic representation of nBABA molecules showing the positions of permanent dipoles.

weak S_C type SRO is expected for $n \leq 3$ which should increase with n as has been observed by us. This would explain the observation that $\xi_{2\perp}$ increases with increasing n. However, this does not explain why $\xi_{2\parallel}$ remains almost independent of n. We feel that at low values of n it is the terminal interactions, responsible for the 1-d correlation, which lead to the relatively large observed value of $\xi_{2\parallel}$ (2 to 3 molecular dimer lengths). But as *n* increases, the interactions responsible for the S_C type order take over (Figure 9) giving rise to a comparable value of $\xi_{2\parallel}$.

The observed decrease of the tilt angle with *n* can be explained in the following way. For $n > 3$ the dipolar interactions perpendicular to $\hat{n}$ hardly change with *n*. This is because $\langle\mu_i\rangle$ varies little for chain lengths greater than the propyl ($n = 3$), and r_{12} ($=$D) is also independent of chain length. However, with increasing chain length the molecules might reposition themselves along $\hat{n}$ in such a way that the chain overlap increases (θ_t decreases) thus increasing the chain–chain interactions. However, the strong dipolar interactions do not allow a large change in the relative positions of the molecules. This would explain the small though finite decrease in θ_t as *n* increases.

CONCLUSIONS

Our x-ray diffraction results with nBABAs have revealed the existence of 1-d correlation of the molecular units along the director in the short range ordered regions in addition to the S_C type order observed in other nematics. The S_C type SRO grows rapidly in strength with increasing *n* for $n > 3$ whereas the strength of the 1-d correlation is maximum for $n = 4$, and becomes negligible for $n > 7$. The values as well as the *n*-dependence of L_{CU}, the length of the 1-d correlated unit, show that the end chains of the molecules are not in an all-trans conformation, in the 1-d correlated strings. The length of the molecular dimer, obtained from the results on S_C type SRO, is greater than L, *the calculated dimer length with the molecule in the extended* zig-zag conformation, which is surprising. This is possible if the 1-d correlated strings and S_C type order exist in different regions, i.e. the 1-d correlated units are not part of the cybotactic groups. This is a model that has also been considered by others.[7]

The observed results can be qualitatively explained, if one assumes (1) the 1-d correlation to be due to large terminal inter-molecular interactions and (2) the S_C-type SRO to originate from the chain–chain (Van der Waals) interactions and also various dipolar interactions between the neighbouring molecules, $\perp$ to $\hat{n}$.

Acknowledgements

We wish to thank C. Manohar, V. K. Kelkar and A. M. Levelut for useful discussions and D. Taupin for helping us to obtain intensity contour maps. We are also grateful to J. N. Soni and his staff for technical help.

References

1. K. Usha Deniz, A. S. Paranjpe, E. B. Mirza, P. S. Parvathanathan and K. S. Patel, *Proc. Nucl. Phys. Solid State Phys. Symp., Poona*, **20C**, 362 (1977).
2. K. Usha Deniz, A. S. Paranjpe, E. B. Mirza, P. S. Parvathanathan and K. S. Patel, *J. Physique*, **40**, C3-136 (1979).
3. A. S. Paranjpe, Ph.D Thesis, University of Bombay (1981).
4. A. de Vries, *Mol. Cryst. Liq. Cryst.*, **10**, 219 (1970).
5. K. Usha Deniz, A. S. Paranjpe, V. Amirthlingam and K. V. Muralidharan, *Mol. Cryst. Liq. Cryst. (Letters)*, **49**, 265 (1979).
   K. Usha Deniz, A. S. Paranjpe, V. Amirthlingam and K. V. Muralidharan, *Liquid Crystals*, Ed. S. Chandrasekhar (Heyden and Sons Ltd.), 185 (1980).
6. This photograph was taken for us by Dr. A. M. Levelut, and we are very thankful to her for the same.
7. B. Zaghloul, Thèse Doctorat de 3^e cycle, Université de Paris-Sud (France), (1984).
8. Jean Doucet, Thèse Doctorat d'État, Université de Paris-Sud (France), (1978).
9. A. de Vries, *Mol. Cryst. Liq. Cryst.*, **11**, 361 (1970).
10. A. J. Leadbetter and E. K. Norris, *Mol. Phys.*, **38**, 669 (1979).
11. A. S. Paranjpe, *Mol. Cryst. Liq. Cryst. (Letters)*, **82**, 93 (1982).
12. A. S. Paranjpe and V. K. Kelkar, *Mol. Cryst. Liq. Cryst. (Letters)*, **102**, 289 (1984).
13. L. V. Azaroff, *Elements of x-ray Crystallography* (McGraw Hill Book Co. Inc., New York, P551 (1968).
14. K. Usha Deniz, E. B. Mirza, U. R. K. Rao, P. S. Parvathanathan, A. S. Paranjpe and A. V. Patankar, *Thermal Analysis*, Vol. I, Ed. Bernard Miller, P796, (1982).
    K. Usha Deniz, E. B. Mirza, P. S. Parvathanathan, A. V. Patnakar and A. S. Paranjpe, *Mol. Cryst. Liq. Cryst.*, **109**, 271 (1984).
15. W. Maier and A. Saupe, *Z. Naturforsch., Teil*, **A15**, 287 (1960).
    W. L. McMillan, *Phys. Rev.* **A4**, 1238 (1971).
16. P. G. De Gennes, *Mol. Cryst. Liq. Cryst.*, **21**, 49 (1976).
17. K. C. Chu and W. L. McMillan, *Phys. Rev.*, **15**, 1181 (1977).
18. Jing-huei Chen and T. C. Lubensky, *Phys. Rev.*, **A14**, 1202 (1976).
19. S. A. Brazowskii, *Sov. Phys. JETP*, **41**, 85 (1975).
20. C. R. Safinya, L. J. Martinez-Miranda, M. Kaplan, J. D. Litster and R. J. Birgeneau, *Phys. Rev. Lett.*, **50**, 56 (1983).
21. A. de Vries, *Liquid Crystals*, Ed. S. Chandrasekhar (Pramana supplement I), P93 (1973).
22. W. L. McMillan, *Phys. Rev.*, **A6**, 936 (1972).
23. W. L. McMillan, *Phys. Rev.*, **A8**, 1921 (1973).
24. B. W. Van der Meer and G. Vertogen, *J. de Phys. colloque C3*, **40**, 223 (1979).
25. J. Charvolin and A. Tardieu, *Solid State Physics Suppl.*, **14** (Liquid Crystals), Ed. L. Liebert P244 (1978).
26. S. K. Paranjpe (private communication).